Biophysical Chemistry 248 (2019) 9–15

Contents lists available at ScienceDirect

Biophysical Chemistry

journal homepage: www.elsevier.com/locate/biophyschem

Single-molecule measurement and bioinformatics analysis suggest a preferred orientation of human coagulation factor VIII on hydrophobic interfaces

Jie Cheng[a,b,d], Feng Geng[c], Jun Hu[a,b], Junhong Lü[a,b,*]

[a] Zhangjiang Lab, Shanghai Advanced Research Institute, Chinese Academy of Sciences, Shanghai 201210, China
[b] CAS Key Laboratory of Interfacial Physics and Technology, Shanghai Institute of Applied Physics, Chinese Academy of Sciences, Shanghai 201800, China
[c] School of Pharmacy, Binzhou Medicine University, Yantai 300064, China
[d] University of Chinese Academy of Sciences, Beijing 100049, China

HIGHLIGHTS

- The height and Young's modulus of individual proteins were measured.
- Protein properties were influenced by the interfacial hydrophilicity/hydrophobicity.
- Human coagulation factor VIII has a preferred orientation on the hydrophobic surface.
- Quantitative nanomechanical mapping and bioinformatics analysis were used.

GRAPHICAL ABSTRACT

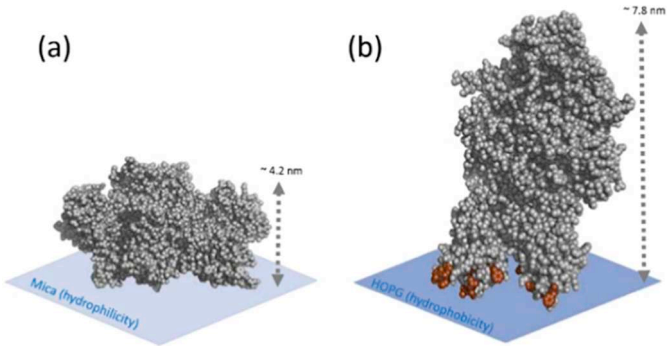

ARTICLE INFO

Keywords:
Blood coagulation protein
Interfacial orientation
Hydrophilicity/hydrophobicity
Atomic force microscope
Single molecule

ABSTRACT

Investigating the adsorption behavior of coagulation proteins on interfaces will contribute to better understating blood clotting and to the development of biocompatible materials. In this work, atomic force microscopy (AFM)-based peakforce quantitative nanomechanical mapping (PF-QNM) was combined with bioinformatics tool to study the adsorption and orientation of coagulation factor VIII (FVIII) on both hydrophilic and hydrophobic interfaces by the height and mechanical measurement of single protein molecules. We found that interfacial hydrophilicity/hydrophobicity greatly influence the heights and Young's modulus of individual proteins. Compared to on the hydrophilic mica surface, FVIII proteins appear bigger vertical sizes while similar lateral sizes on the HOPG surface. The water accessible surface area analysis indicate stronger apolar properties C1 and C2 domains than others, suggesting a preferred orientation through the strong hydrophobic interactions between HOPG and the hydrophobic residues interface of the protein domains. These results provide novel insights on the adsorption and binding mechanism of the FVIII on cell membrane and will be helpful for the design of anticoagulant materials.

* Corresponding author at: Zhangjiang Lab, Shanghai Advanced Research Institute, Chinese Academy of Sciences, Shanghai 201210, China.
E-mail address: lujunhong@sinap.ac.cn (J. Lü).

https://doi.org/10.1016/j.bpc.2019.03.001
Received 5 February 2019; Received in revised form 4 March 2019; Accepted 13 March 2019
Available online 15 March 2019

1. Introduction

The adsorption behavior of proteins, such as plasma proteins, fibrinogen and globulin, on the cellular interface can activate a series of clotting factors and coagulation reactions, which is a common phenomenon in the biological processes [1–3]. Meanwhile the protein adsorption on the biomaterial interfaces usually induce kinds of foreign body reactions, including inflammations, immunities and adhesions of bacteria, which greatly hamper the application of biomaterials in clinic medicine [4–8]. Therefore, it is required to understand, predict and control the adsorption behaviours of the proteins on interfaces for improving their performances in biomedical materials, biosensors, enzyme engineering and regenerative medicines, especially proteins participated in reactions of blood coagulation cascades [9,10].

Coagulation factor VIII (FVIII) is one of the clotting cofactors released in coagulation cascade reaction when a blood vessel is injured. Naturally, the structure of FVIII is a heterodimer, which is composed of two non-covalent linked polypeptide chains: a heavy chain (HC) of 90–220 kDa (A1-A2-B) and a light chain (LC) of 80 kDa (A3-C1-C2) [11–14]. The two C domains from the light chain are capable of binding phospholipid membrane: the C2 domain binds to phosphatidylserine-containing membranes through hydrophobic spikes by the hydrophobic residues (Met 2199/Phe 2200 and Leu 2251/Leu 2252), while the C1 domain binds the membranes by residues Lys 2092/Phe 2093 and Ile 2158/Arg 2159 in which Phe 2093 and Ile 2158 are hydrophobic [15–18]. In vivo, FVIII is stabilized by binding to von Willebrand factor (vWF). In the coagulation reaction, FVIII transforms from the inactive state into the active one (FVIIIa) by thrombin. FVIIIa is dissociated from vWF by the cleavage at 1689, permitting the interaction of FVIIIa with platelets. Accompanying with conformation changes of FVIIIa, it initiates the downstream reactions together with the coagulation factors IX (FIXa), calcium ions (Ca^{2+}) and phospholipid membranes. In a clotting process, the adsorption of FVIII on the phospholipid membrane which is a complex interface for the reaction, is an essential step to activate the coagulation reaction [19]. Previous data have shown that the low adsorption of FVIII on the phospholipid membrane leads to the failure of clotting processes, which is the main reason of hemophilia A [20]. Unfortunately, the mechanism of the adsorption process of FVIII on the membrane is still unclear. Therefore, it is important to study of the interaction between FVIII and the membrane for a better understanding of the processes of the coagulation reaction and the function of the blood coagulation proteins.

Atomic force microscopy (AFM) has been widely used to examine the adsorption behaviours of biomolecules on the interfaces at the single-molecule level [4,21–23]. With recently development of the peakforce quantitative nanomechanical mapping (PF-QNM), it is possible to map the protein topography and Young's modulus with a high spatial resolution either in air or liquid environment [24]. The Young's modulus is a mechanical property that shows a material's stiffness to elastic deformation under lode. When the lode is removed, the material returns to its original shape. It relates the relationship between stress and strain in a material along an axis or line. So more deformation occurs in a flexible material like proteins. Agnieszka et al. used PF-QNM to measure elastic modulus of the single human immunoglobulin M antibody, the results yielded a low elastic modulus of about 34 ± 10 MPa [24]. The measured Young's modulus of bovine carbonic anhydrase II progressively decreased from 75 MPa to 20 MPa as the denaturant concentration was increased [25]. With the differences in packing density among and between fibrils, the observed Young's modulus has a large range from 1 MPa to tens of MPa [26]. Since the adsorption processes of the proteins on interfaces are often accompanied with the conformation or orientation changes, PF-QNM is an effective measurement to study the interfacial adsorption behaviours of the proteins on different surfaces.

In this work, we have applied AFM-based PF-QNM technique to investigate the height of single FVIII protein molecules on the mica and highly oriented pyrolytic graphite (HOPG) surfaces, respectively. The mica and HOPG have similar atomic-grade flatness and roughness surfaces which lead to slight influence to the adsorption of FVIII. However, mica and HOPG show apparently different characters of hydrophobicity and the electrical properties. In brief, mica has a hydrophilic surface interface is with negatively charge while HOPG is electrically neutral with a hydrophobic surface. By the combination of hydrophilicity analysis of the protein and its domains, we demonstrated that the hydrophobic interaction between protein domains and HOPG determine a specific orientation and mechanical properties of FVIII proteins.

2. Materials and methods

2.1. Sample preparation

Protein samples consisting of a freeze-dried preparation of plasma-derived human protein coagulation Factor VIII and tris-buffered saline (TBS, pH = 7.6) (10×) were purchased from Sigma-Aldrich. The 1× TBS buffer was used to dissolve FVIII, which was diluted by ultrapure water. A 20 uL drop of 20–60 μg/ml FVIII solution was placed on the interface of either freshly cleaved mica or HOPG for protein deposition and then the sample was rinsed by 1× TBS buffer.

2.2. Dynamic light scattering (DLS)

FVIII solutions was evaluated using a Zetasizer Nano ZS90 apparatus (Malvern, Worcestershire, UK). The apparatus was equilibrated at 25 °C and 1 mL of formulations were analysed using a plastic cuvette under the automatic mode to identify the size. Each sample was measured 3 times with an intervening interval of 30 s. Zeta average radius was calculated from the auto-correlated function using Zetasizer software version 7.11 (Malvern Instruments).

2.3. Atomic force microscopy (AFM)-based height and mechanical measurement

The AFM experiments were carried out on NanoScope VIII equipped with a "J" scanner (125 μm × 125 μm). Silicon nitride probes (D-NPS) with spring constants of ~0.35 N/m were used in all measurements. All experiments were conducted in TBS buffer by a commercially available fluid cell which was washed before used. The imaging mode was the tapping mode and the peakforce quantitative nanomechanical mapping mode (PF-QNM). In the PF-QNM mode, the calibration procedure has been completed before the mechanical measurement. The deflection sensitivity was calibrated by a PF-QNM ramp, after which the spring constant of the cantilever was calibrated via thermal tuning. The calibration of the deflection sensitivity and spring constant were carefully performed. The elastic modulus for the samples was calculated by the Derjaguin-Muller-Toporov (DMT) model [27].

All images were recorded at 256 pixels × 256 pixels. The frequency of the peak force was 1 kHz and the scan rate was 1 Hz. NanoScope Analysis software were used for analysis. The topography images shown in this work were handled with a line-wise 2st order flattening while modulus maps were rendered from the raw data with no treatment. The distribution of height and modulus derived from the AFM mapping and fitted by Gaussian distribution using origin software.

2.4. Bioinformatics analysis of the hydrophilic and hydrophobic properties of FVIII proteins

According to Kyte and Doolittle method (K-D method) [28], nine hydrophilic amino acids (arginine (Arg), lysine (Lys), histidine (His), glutamic acid (Glu), aspartic acid (Asp), asparagine (Asn), glutamine (Gln), proline (Pro), tyrosine (Tyr)), and eight hydrophobic amino acids (isoleucine (Ile), valine (Val), leucine (Leu), proline (Phe), cysteine

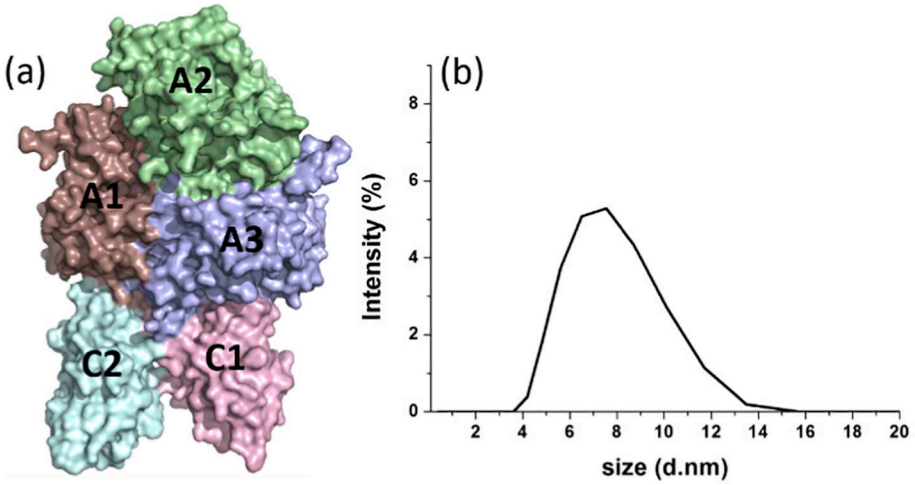

Fig. 1. (a) The crystal structure of FVIII (PDB ID: 3CDZ) with showing the domains. (b) Size distribution by volume of FVIII measured by dynamic light scattering.

(Cys), methionine (Met), alanine (Ala) and glycine (Gly)) were chosen to evaluate the hydrophilic and hydrophobic performance of FVIII and each domain. The crystal structure was prepared using the program PyMOL by coloring according to the CPK scheme. The solvent accessible surface areas (ASA) for the full FVIII proteins and its domains were estimated at The PDBePISA server (www.pdbe.org/pisa) [29].

3. Results and discussion

The natural human full-length FVIII consists of six domains described as A1-A2-B-A3-C1-C2. However, currently available crystal structures are B-domain depleted recombinant FVIII (Fig. 1a). In this work, plasma-derived human full-length coagulation FVIII was used. We first check protein samples by dynamic light scattering (DLS) to measure the size of individual proteins in solution. The DLS result shows that FVIIII proteins present a single-molecule distribution with the average particle sizes of about ~7.5 nm (Fig. 1b).

The adsorption behaviour of FVIII protein molecules on the freshly cleaved mica and HOPG are firstly studied in air condition using the tapping mode AFM, respectively. The representative topography images (Fig. 2a and c) show that single FVIII molecules are generally spherical shape, which is in agreement with other work [30–33]. Interestingly, the vertical heights of FVIII proteins both on mica and HOPG reveal a typical uniform structure with one Gaussian curve. The heights of FVIIIs on the mica range from 1.8 nm to 2.0 nm with a peak value of 1.9 nm from Gaussian fitting (Fig. 2b), while the heights of the FVIIIs on the HOPG are between 3.3 nm and 4.1 nm with a peak value of 3.8 nm (Fig. 2d). These results show that the average height of FVIIIs on the mica is only half of that on the HOPG (Fig. 2), both of which are lower than the theoretical values [34]. These may be attributed to the atmospheric environment, which is usually lead to unexpected dehydration of the proteins, formation of salt layers on the interface and the complex interactions between the tip and the sample.

To rule out the possible adverse effects of the atmospheric environments on the protein structures, FVIII samples are imaged in the liquid buffer. As shown in Fig. 3, FVIII proteins are dispersed well with single particles on either the mica or HOPG surfaces. The Gaussian fitting statistical analysis of the heights of FVIII shows a distribution in the region of 3.4 nm to 4.9 nm on the mica with a peak value of 4.2 nm (Fig. 3b) while a height distribution between 7.1 nm and 8.7 nm on the HOPG interface (the peak value is 7.8 nm, Fig. 3d). The apparent height of FVIII on the HOPG is 1.9 times as high as that on the mica.

The mechanical properties of FVIII on different interfaces (mica /HOPG) have also been investigated by PF-QNM. After Gaussian fitting, we found that the Young's modulus of proteins slightly vary on different interfaces. The Young's modulus of FVIII on the mica distribute from 1.9 MPa to 5.1 MPa, with two peak values of 2.7 MPa and 4.2 MPa (Fig. 4b), while the Young's modulus of FVIII on HOPG spread within the range of 1.7 MPa to 3.6 MPa, and the peak value is 2.4 MPa (Fig. 4d). On hydrophilic interface, the higher degree of freedom of the proteins leads to the non-uniform mechanical properties of FVIII, which results two different peaks in the Gaussian distributions of FVIII on the mica (Fig. 4b). On the other hand, the strong interaction between FVIII and the hydrophobic interface makes the orientation of FVIII on HOPG consistent with a unique Young's modulus (Fig. 4d). As a result, FVIII exhibits apparently higher height and lower Young's modulus on the HOPG interface with the hydrophobic character.

In general, the adsorption behaviours of proteins on the similar atomic-grade flatness and roughness surfaces may be influenced mainly by the hydrophobicity and the electrostatic properties of the interfaces [35]. Although the surfaces of FVIII and mica are both negatively charged and the surface of HOPG is electrically neutral, these electrical properties, especially the mutual repulsive force between the interfaces of mica and FVIII, are not strong enough to shift the equilibrium in the solution and affect in the adsorption behaviour of proteins on different interfaces [32,36].

On a hydrophilic surface, such as mica, the electrostatic interaction by hydrophilicity is the main force between protein and substrate surface, although it might also be weakly affected by the equilibrium ions in the solution. After the proteins attached to the surfaces, the hydrophilic groups and the surface charges of proteins attract water molecules to form hydration shell and to maintain their stability [37]. The amino acid side chains with relatively strong hydrophilicity on the protein interface would mainly interact with the mica surface with electrostatic forces] [30,36], resulting in a flexible orientation of FVIIIs on the mica (Figs. 2–3).

On the hydrophobic HOPG surface, however, the adsorption and orientation of proteins shows distinct conditions. Naturally, the folded proteins in solution tend to maintain their tertiary structures with hiding hydrophobic nonpolar residues inside the molecules [34]. After adsorption on a hydrophobic substrate, the hydrophobic groups within the protein and the water molecules nearby would be rearranged [30–32]. The hydrogen bonds encircled the hydrophobic groups may be formed between the protein and the substrate, which limits the orientation and flexibility of the proteins through the space steric hindrances.

In the case of protein FVIII, the distribution of hydrophilic and hydrophobic amino acids on their surfaces have been analysed by space-filling display of FVIII crystal structure according to the CPK scheme. The same as we inferred, as shown in Fig. 5a–b, the hydrophilic

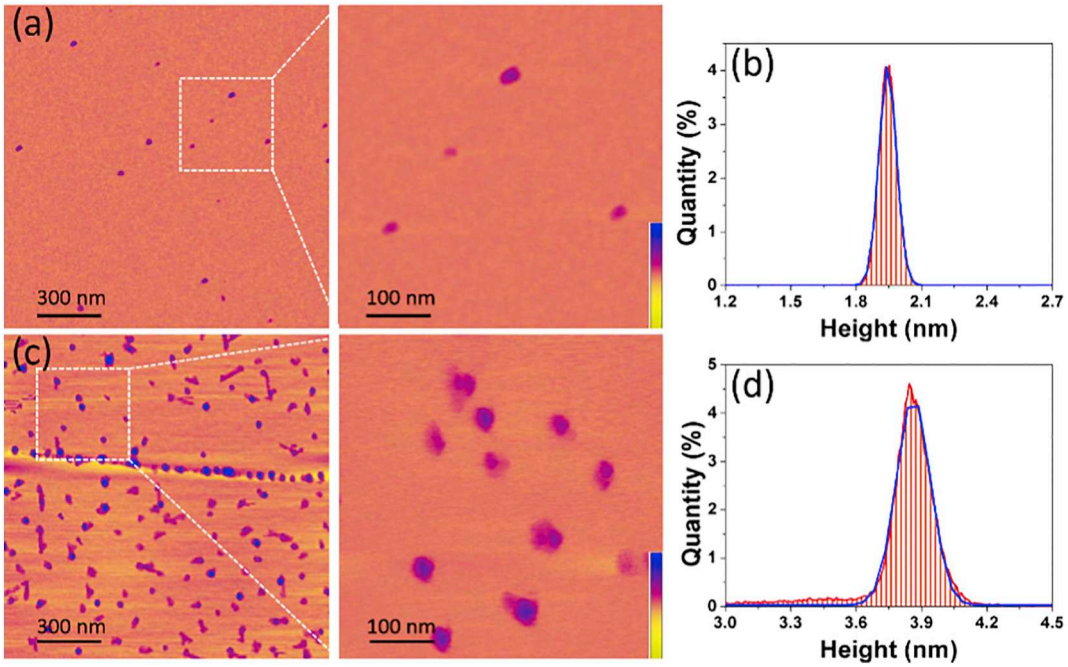

Fig. 2. Tapping mode AFM images of FVIII proteins on hydrophilic (mica) and hydrophobic (HOPG) interfaces in air condition. (a) The topography images and (b) the height histogram of protein on mica surface, (c) the topography images and (d) the height histogram of protein on HOPG surface. Continuous red lines represent the total fittings (95% confidence bonds); corresponding single Gaussian curves are indicated by blue lines. Colour scale: 10 nm. (For interpretation of the references to colour in this figure legend, the reader is referred to the web version of this article.)

amino acids tend to distribute on the surface, while hydrophobic amino acids mostly hide inside the molecules. Moreover, the proportions of hydrophobic amino acids (isoleucine (Ile), valine (Val), leucine (Leu), proline (Phe), cysteine (Cys), methionine (Met), alanine (Ala), glycine (Gly)) in FVIII and each domain have been analysed based on the hydrophobic parameters of amino acids from the Kyte and Doolittle method (K-D method) [28]. The results indicate that 40.1% of the amino acids are hydrophobic in FVIII (Fig. 5c), most of which hide

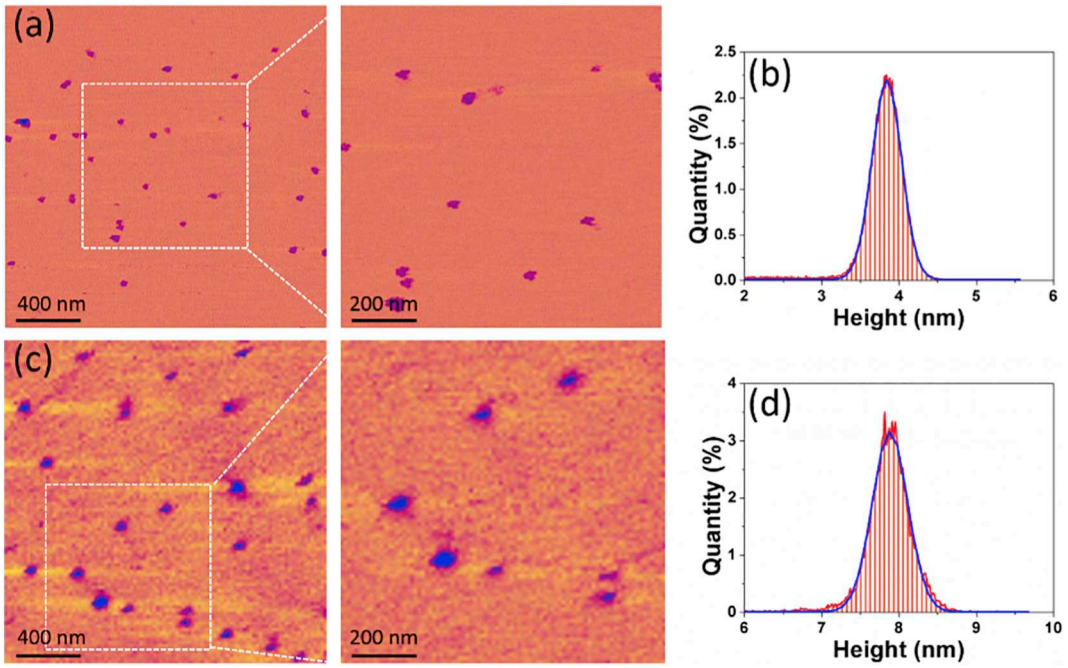

Fig. 3. PF-QNM AFM images of FVIII proteins on hydrophilic (mica) and hydrophobic (HOPG) interfaces in liquid condition. (a) The topography images and (b) the height histogram of proteins on mica surface, (c) the topography images and (d) the height histogram of proteins on HOPG surface. Continuous red lines represent the total fittings (95% confidence bonds); corresponding single Gaussian curves are indicated by blue lines. Colour scale: 10 nm. (For interpretation of the references to colour in this figure legend, the reader is referred to the web version of this article.)

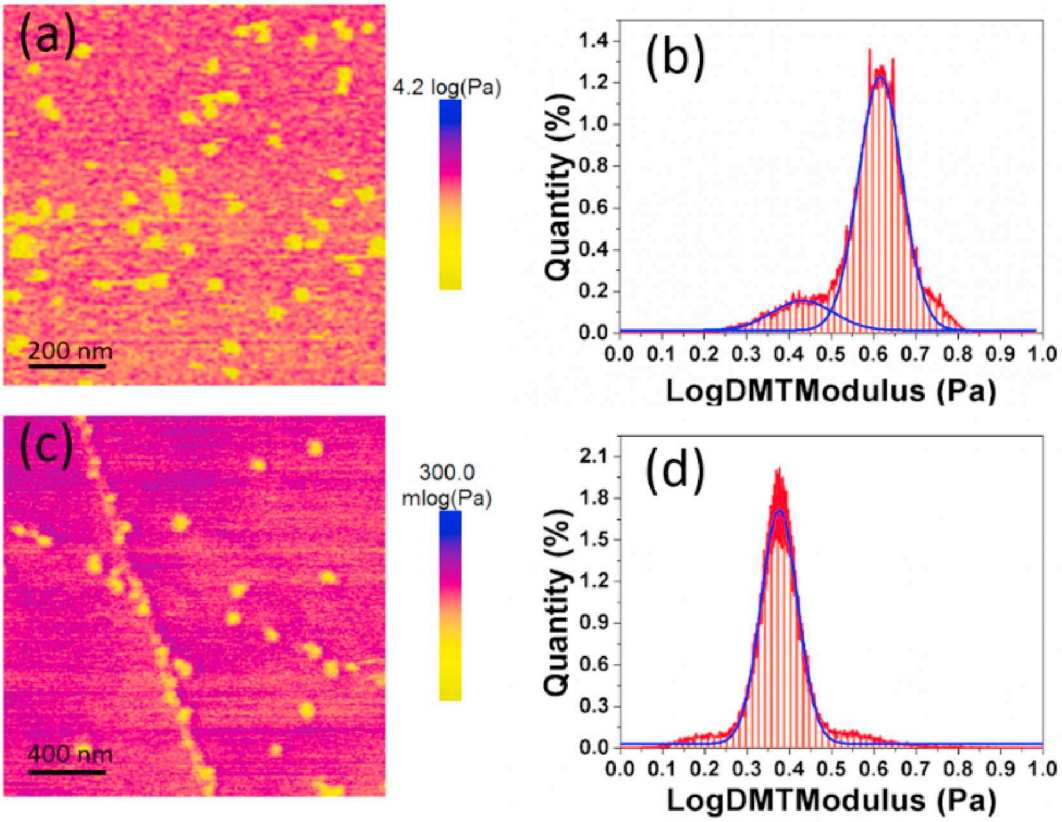

Fig. 4. The modulus of FVIII proteins on hydrophilic (mica) and hydrophobic (HOPG) interfaces in liquid condition. The effective elastic modulus images of proteins on mica(a) and on HOPG(c).The histogram of the values on mica(a) and on HOPG(c) are given in (b) and (d),respectively. Continuous red lines represent the total fittings (95% confidence bonds); corresponding single Gaussian curves are indicated by blue lines. (For interpretation of the references to colour in this figure legend, the reader is referred to the web version of this article.)

inside the molecule, in contrast the other hydrophilic amino acids tend to expose on the surface from the three-dimensional structure of FVIII (Fig. 5a–b). The ratio of hydrophobic amino acids in each domain is C1 > A1 > C2 > A2 > A3. Among them, the proportion of hydrophobic amino acids in C1 domain is the highest, reaching to 45.5%, followed by A1 and C2 domains, which are 44.3% and 41.0%, respectively (Fig. 5c). The water accessible surface area (ASA) of FVIII domains were also further analysed by PDBePISA server [29]. As shown in Fig. 5C, the ASA of C1 and C2 domains (7319.0 $Å^2$ and 8049.8 $Å^2$, respectively) are significant smaller than these of other domains (15,011.5 $Å^2$, 16,221.6 $Å^2$ and 15,901.4 $Å^2$, according to A1, A2, A3 domains, respectively) and the full protein (56,120.0$Å^2$). The smaller ASA means that C1 and C2 domain surfaces present stronger apolar properties, which maybe attribute to the high percent of hydrophobic amino acids in the two domains. Previous researches have proved that the hydrophobic residues on the two C domains contribute to phospholipid membrane binding [17,18,38]. These hydrophobic spikes on C2 domain can penetrate hydrophobic core of a phospholipid bilayer and bind to phospholipid membranes. Mutation of the hydrophobic spike amino acids both in C1 and C2 domains may have a reduced affinity for phospholipid [17,38].

Based on the above results, we speculate that FVIII tend to interact with the hydrophobic interface by the hydrophobic amino acids from C1 and C2 domains on the HOPG surface (Fig. 6), which leads to a preferred orientation. Therefore, there is no surprise to obtain the apparently different heights on different interface: the hydrophobic interaction between the interface and the protein made the height of FVIII on HOPG 1.9 times as high as that on mica. In the blood, FVIII is proteolytically activated by thrombin. During the activation process, specific cleavage sites are recognized by thrombin. Upon adsorption on the interface, the changed orientation of FVIII maybe influence the binding site and proteolytic activity of thrombin, thus impacting the following catalytic efficiency of FXa [39]. The manner in which material surface or membrane engagement alters the orientation or conformation of factor VIII is an interesting topic for further investigation.

4. Conclusions

In this work, the orientations of FVIII on different interfaces (mica /HOPG) have been studied in the air/liquid environment using the high-resolution AFM method by the height and mechanical measurement of single proteins. The AFM result show that the apparent height of FVIII on the mica interface is significantly lower than that on the HOPG in both conditions while the Young's modulus on the mica interface is higher than that on HOPG. Bioinformatics analysis further revealed that the C1 and C2 domain have more hydrophobic amino acids on their interface. These results suggested that the weak electrostatic force as the main interaction between protein and the hydrophilic interface lead to a random orientation on the mica surface, while the strong hydrophobic interaction as the main force between FVIII C1 and C2 domain and the hydrophobic interface results in a preferred orientation on the HOPG surface. Thus, this study provides a theoretical support for the design of the anticoagulant materials and lays a foundation to investigate the interactions between prothrombin and phospholipid membranes.

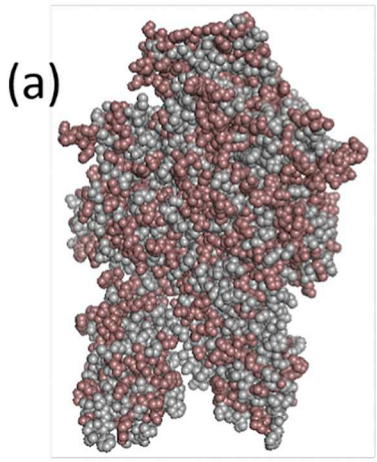

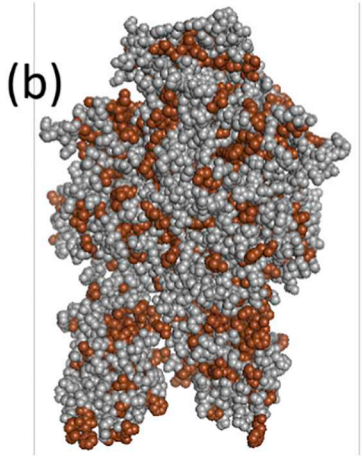

(c)

Domains	FVIII	A1	A2	A3	C1	C2
Proportion of hydrophobic amino acids (%)	40.1	43.3	39.8	37.3	45.5	41.0
Accessible surface areas (Å²)	56120.0	15011.5	16221.6	15901.4	7319.0	8049.8

Fig. 5. Hydrophobicity and accessible surface area analysis of amino acids within FVIII protein and each domains. The distribution of hydrophilic amino acids (a) and hydrophobic amino acids (b) on the FVIII protein interface, (c) the proportion of hydrophobic amino acids and accessible surface area in the whole FVIII protein and each domains. Space-filling display of the factor VIII crystal structure (PDB ID: 3CDZ). Light and dark brown represent hydrophilic and hydrophobic amino acids, respectively. (For interpretation of the references to colour in this figure legend, the reader is referred to the web version of this article.)

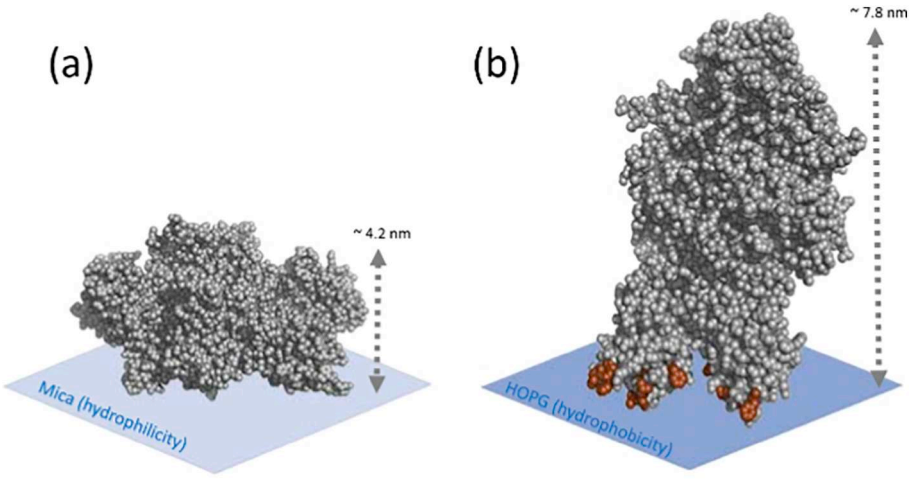

Fig. 6. Schematic diagram of a FVIII protein on hydrophilic (mica) and hydrophobic (HOPG) interfaces. Space-filling display of the factor VIII crystal structure (PDB ID: 3CDZ). Dark brown represents hydrophobic amino acids. (For interpretation of the references to colour in this figure legend, the reader is referred to the web version of this article.)

Acknowledgements

This work was supported by National Natural Science Foundation of China [Nos.11474298 and U1732130]; Key Research Program of Frontier Sciences of the Chinese Academy of Sciences [QYZDJ-SSW-SLH019]; Natural Science Foundation of Shandong Province [ZR2017LC006]; and the Scientific Research Foundation of Binzhou Medical University [BY2017KYQD02].

References

[1] M. Hoffman, Remodeling the blood coagulation Cascade, J. Thromb. Thrombolysis 16 (2003) 17–20.
[2] S. Monica, B.C. Furie, F. Bruce, The blood coagulation cascade, Curr. Opin. Hematol. 11 (2004) 272–277.
[3] W. Kyung Mi, S. Jihye, Z. Ruiyun, P.X. Ma, Suppression of apoptosis by enhanced protein adsorption on polymer/hydroxyapatite composite scaffolds, Biomaterials 28 (2007) 2622–2630.
[4] N.A. Barinov, V.V. Prokhorov, E.V. Dubrovin, D.V. Klinov, AFM visualization at a single-molecule level of denaturated states of proteins on graphite, Colloids Surf. B: Biointerfaces 146 (2016) 777–784.
[5] L. Manping, W. Huaiyu, R. Changshun, X. Juan, W. Jinfeng, L. Yan, W. Yuanliang, L. Yanfeng, Adsorption force of fibronectin on various surface chemistries and its vital role in osteoblast adhesion, Biomacromolecules 16 (2015) 973–984.
[6] S. Claudia, F. Marion, M.F. Maitz, W. Carsten, Blood coagulation on biomaterials requires the combination of distinct activation processes, Biomaterials 30 (2009) 4447–4456.
[7] L. Martin, S. Ingmar, J. Bengt-Harald, Protein adsorption onto silica nanoparticles: conformational changes depend on the particles' curvature and the protein stability,

Langmuir the Acs, J. Surf. Colloids 20 (2009) 10639.
[8] X. Peng, H. Fu, R. Liu, L. Zhao, Y. Zu, F. Xu, Z. Liu, Adsorption of human serum albumin onto highly orientated pyrolytic graphite surface studied by atomic force microscopy, Scanning 37 (2015) 158–164.
[9] L. Andréas, E. Tobias, A. Olof, L. Bo, Photografted poly(ethylene glycol) matrix for affinity interaction studies, Biomacromolecules 8 (2007) 287–295.
[10] S. Theodora Tsapikouni, F. Yannis Missirlis, Protein-material interactions: from micro-to-nano scale, Mater. Sci. Eng. B 152 (2008) 2–7.
[11] J. Gitschier, W.I. Wood, T.M. Goralka, K.L. Wion, E.Y. Chen, D.H. Eaton, G.A. Vehar, D.J. Capon, R.M. Lawn, Characterization of the human factor VIII gene, Nature 312 (1984) 326–330.
[12] P.J. Fay, Factor VIII structure and function, Int. J. Hematol. 83 (2006) 103–108.
[13] P.J. Fay, P.V. Jenkins, Mutating factor VIII: lessons from structure to function, Blood Rev. 19 (2005) 15–27.
[14] W. Wang, Y.J. Wang, D.N. Kelner, Coagulation factor VIII: structure and stability, Int. J. Pharm. 259 (2003) 1–15.
[15] E. Hanna, L. Svenja, D. Ingmar, R.R. Netz, J.O. Rädler, FVIII binding to PS membranes differs in the activated and non-activated form and can be shielded by annexin A5, J. Phys. Chem. B 115 (2011) 12963–12970.
[16] S.M. Svetla, B.O. Villoutreix, M. Koen, K.C. Geoffrey, H. Andreas, 3-Dimensional structure of membrane-bound coagulation factor VIII: modeling of the factor VIII heterodimer within a 3-dimensional density map derived by electron crystallography, Blood 99 (2002) 1215–1223.
[17] G.E. Gilbert, R.J. Kaufman, A.A. Arena, M. Hongzhi, S.W. Pipe, Four hydrophobic amino acids of the factor VIII C2 domain are constituents of both the membrane-binding and von Willebrand factor-binding motifs, J. Biol. Chem. 277 (2002) 6374.
[18] B. Esther, V.D.B. Maartje, W. Aleksandra, V. Jan, J.H. Faber, K. Marianne, H.R. Stennicke, M. Koen, A.B. Meijer, Factor VIII C1 domain spikes 2092-2093 and 2158-2159 comprise regions that modulate cofactor function and cellular uptake, J. Biol. Chem. 288 (2013) 29670–29679.
[19] V.J. Bom, R.M. Bertina, The contributions of Ca2+, phospholipids and tissue-factor apoprotein to the activation of human blood-coagulation factor X by activated factor VII, Biochem. J. 265 (1990) 327.
[20] S.E. Antonarakis, J.P. Rossiter, M. Young, J. Horst, P.D. Moerloose, S.S. Sommer, R.P. Ketterling, H.J. Kazazian, C. Negrier, C. Vinciguerra, Factor VIII gene inversions in severe hemophilia A: results of an international consortium study, Blood 86 (1995) 2206–2212.
[21] Y. Kamiya, K. Yamazaki, T. Ogino, Protein adsorption to graphene surfaces controlled by chemical modification of the substrate surfaces, J. Colloid Interface Sci. 431 (2014) 77–81.
[22] S.J. Haward, P.R. Shewry, M.J. Miles, T.J. Mcmaster, Direct real-time imaging of protein adsorption onto hydrophilic and hydrophobic surfaces, Biopolymers 93 (2010) 74–84.
[23] R.T. Gettens, Z. Bai, J.L. Gilbert, Quantification of the kinetics and thermodynamics of protein adsorption using atomic force microscopy, J. Biomed. Mater. Res. A 72A (2005) 246–257.
[24] A. Voss, C. Dietz, A. Stocker, R.W. Stark, Quantitative measurement of the mechanical properties of human antibodies with sub-10-nm resolution in a liquid environment, Nano Res. 8 (2015) 1987–1996.
[25] N.E. Kurland, Z. Drira, V.K. Yadavalli, Measurement of nanomechanical properties of biomolecules using atomic force microscopy, Micron 43 (2012) 116–128.
[26] G. Senli, B.B. Akhremitchev, Packing density and structural heterogeneity of insulin amyloid fibrils measured by AFM nanoindentation, Biomacromolecules 7 (2006) 1630–1636.
[27] B.V. Derjaguin, V.M. Muller, Y.P. Toporov, Effect of contact deformations on the adhesion of particles, J. Colloid Interface Sci. 53 (1975) 314–326.
[28] J. Kyte, R.F. Doolittle, A simple method for displaying the hydropathic character of a protein ☆, J. Mol. Biol. 157 (1982) 105–132.
[29] E.B. Krissinel, K. Henrick, Inference of macromolecular assemblies from crystalline state, J. Mol. Biol. 372 (2007) 774–797.
[30] J. Omkar, M.G. Joseph, D.Q. Wang, Adsorption and function of recombinant factor VIII at solid-water interfaces in the presence of Tween-80, J. Pharm. Sci. 98 (2009) 3099–3107.
[31] W.D. Gray, Honors College Thesis, Oregon State University, 2009.
[32] Y.C. Tai, J. Mcguire, O. Joshi, D.Q. Wang, Solid surface chemical and physical effects on the adsorption of recombinant factor VIII, Pharm. Dev. Technol. 14 (2009) 129–133.
[33] K. Bonazza, H. Rottensteiner, G. Schrenk, C. Fiedler, F. Scheiflinger, G. Allmaier, P.L. Turecek, G. Friedbacher, Ca2+ concentration-dependent conformational change of FVIII B-domain observed by atomic force microscopy, Anal. Bioanal. Chem. 407 (2015) 6051–6056.
[34] W.E. Fowler, P.J. Fay, D.S. Arvan, V.J. Marder, Electron microscopy of human factor V and factor VIII: correlation of morphology with domain structure and localization of factor V activation fragments, Proc. Natl. Acad. Sci. U. S. A. 87 (1990) 7648–7652.
[35] W. Norde, F. Macritchie, G. Nowicka, J. Lyklema, Protein adsorption at solid-liquid interfaces: reversibility and conformation aspects ☆, J. Colloid Interface Sci. 112 (1987) 447–456.
[36] J.R. Wendorf, C.J. Radke, H.W. Blanch, The role of electrolytes on protein adsorption at a hydrophilic solid–water interface, Colloids Surf. B: Biointerfaces 75 (2010) 100–106.
[37] A.G. Richter, K. Ivan, Using in situ X-ray reflectivity to study protein adsorption on hydrophilic and hydrophobic surfaces: benefits and limitations, Langmuir 29 (2013) 5167–5180.
[38] H. Meems, M. van den Biggelaar, M. Rondaij, C. van der Zwaan, K. Mertens, A.B. Meijer, C1 domain residues Lys 2092 and Phe 2093 are of major importance for the endocytic uptake of coagulation factor VIII, Int. J. Biochem. Cell Biol. 43 (2011) 1114–1121.
[39] G. Van Dieijen, G. Tans, J. Rosing, H.C. Hemker, The role of phospholipid and factor VIIIa in the activation of bovine factor X, J. Biol. Chem. 256 (1981) 3433.